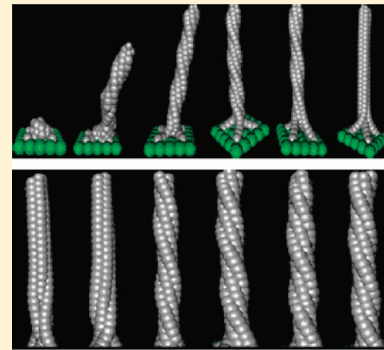


# Self-Assembly of Semiflexible Homopolymers into Helical Bundles: A Brownian Dynamics Simulation Study

Tongtao Yue and Xianren Zhang\*

Division of Molecular and Materials Simulation, State Key Laboratory of Organic-Inorganic Composites, Beijing University of Chemical Technology, Beijing 100029, China

**ABSTRACT:** The controllable self-assembly of semiflexible homopolymers into regular bundles has received much attention because of its potential importance in various fields, such as the storage of elastic energy, the fabrication of nanostructures, and the formation of the cytoskeleton in living cells. In this article, using computer simulations, we investigate how semiflexible homopolymers anchored on a substrate self-organize into ordered structures, focusing on both the patterns formed and the dynamics of self-assembly. For the self-assembly pattern, four different patterns, including patterns with unclustered polymers, disordered semispherical clusters, highly ordered helical bundles, and parallel bundles, are observed from our simulations. The formation of stable bundles requires semiflexible homopolymers having a sufficient molecule length and intermediate bending stiffness, whereas the formation of the helical structures depends on the balance between the inter-homopolymer attraction and the bending stiffness of homopolymers. Furthermore, the bundle formation reinforces the bending stiffness, and the stiffness is further enhanced by the helical bundling. For the dynamic aspect, both hierarchical bundling and nonhierarchical bundling are observed from our simulations.



## 1. INTRODUCTION

Helical structures with various functions and applications are ubiquitous in nature and in our daily life. Helices are especially abundant in biology, with examples including DNA helices, amino acids, mollusk shells, cellulose fibrils in wood,<sup>1</sup> hierarchy in bone,<sup>2,3</sup> chirally spinning nodal cilia,<sup>4</sup> amyloid fibers,<sup>5</sup> and actin filaments.<sup>6</sup> Owing to the essential roles of these structures, understanding the mechanism of helix formation is of both theoretical and technological significance.

In recent years, experimental and theoretical investigations have been performed to explore the formation mechanism of helical structures.<sup>7–19</sup> Theoretically, Chouaieb et al. gave a simple classification of all helical equilibria of inextensible uniform rods.<sup>7</sup> Anisotropic surface stresses<sup>8</sup> and entropy<sup>9,13</sup> were shown to induce the formation of helical structures. Strong space confinement was found to be another driving force for the spontaneous formation of helical structures.<sup>14–18</sup> As a result of tight packing, biomolecules in a crowded environment frequently adopt ordered, helical conformations.<sup>9,11,13</sup> Using a computer simulation method, Kudlay et al.<sup>11</sup> investigated the transition of flexible helical homopolymer like RNA and proteins from random coil to helical structure.

For biopolymers, the formation of helical structure is often involved with the bundling of biopolymers. Although biopolymers with different stiffnesses are abundant in living cells and play vital roles in various cellular activities, in many cases, a single polymer does not function correctly without bundling. A well-known example is actin filaments (F-actin), the main component of the cytoskeleton. Actin filaments always are cross-linked by

actin-binding proteins to form various types of filament bundles,<sup>20</sup> which are tightly bound to the substrate in moving cells.<sup>21–24</sup> In these systems, both the morphology and kinetics of actin bundling are significantly affected by the protein cross-linkers.<sup>25–31</sup> In addition, Grason and Bruinsma argued that the chirality of biopolymers is another key thermodynamic parameter to control the bundling of biopolymers.<sup>32</sup>

Recent research demonstrated that the assembly of nanoscale fibers into helical structures can give rise to the structure of helical bundles.<sup>33–36</sup> Pokroy et al.<sup>33</sup> have investigated the self-organization of mesoscale bristles into helical clusters. They demonstrated that the aggregation process can be finely tuned to yield helical assemblies with a controlled size, pattern, hierarchy, and handedness over large areas. Recently, the same group suggested that the shape and size of nanopillar assembly can be controlled by an adhesion-mediated elastocapillary interaction.<sup>34</sup>

Though the self-organization of mesoscale fibers has been investigated both experimentally and theoretically,<sup>33–36</sup> the mechanism of helical bundling is still not thoroughly understood. Inspired by these works, we investigated here the self-assembly of semiflexible homopolymers anchored on a substrate using a Brownian dynamics (BD) simulation technique at a coarse-grained level. For the self-assembly pattern, four different patterns, including patterns with unclustered polymers, disordered semispherical clusters, highly ordered helical bundles, and parallel

**Received:** April 20, 2011

**Revised:** September 10, 2011

**Published:** September 12, 2011

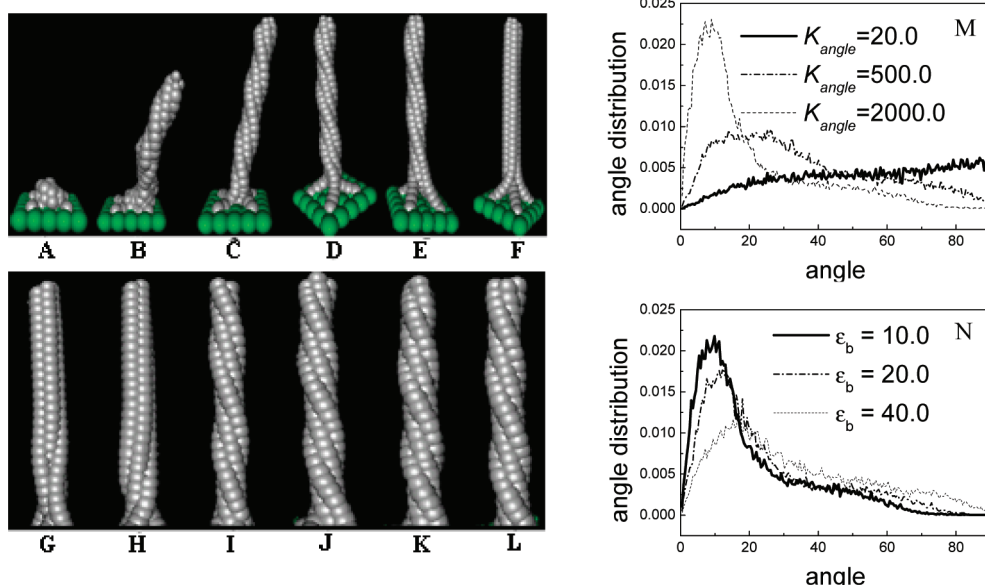


**Figure 1.** (Top) typical snapshots for semiflexible homopolymer molecules with different values of intrinsic bending stiffness,  $K_{\text{angle}}$ : (A) 20.0, (B) 60.0, (C) 200.0, (D) 500.0, (E) 1000.0, and (F) 2000, while  $\epsilon_b$  was set to 60.0. (Bottom) typical snapshots corresponding to four different values of  $\epsilon_b$ : (G) 10.0, (H) 20.0, (I) 40.0, (J) 60.0, (K) 80.0, and (L) 100.0, while  $K_{\text{angle}}$  was fixed to 500.0. (M) and (N) show corresponding distributions of the angle between the bond connecting two neighboring beads and the z-axis for the effects of  $K_{\text{angle}}$  and those of  $\epsilon_b$ , respectively.

bundles, were observed from our simulations. The equilibrium structures formed are found to be controlled by the intrinsic features of semiflexible homopolymers, such as molecule length, intrinsic bending stiffness, and inter-homopolymer attraction. For the assembly dynamics, our simulations show both hierarchical bundling and nonhierarchical bundling, again depending on the intrinsic features of homopolymers. This article is arranged as follows. In Section 2, we describe the model and BD simulation method. Then, the simulation results are presented and discussed in Section 3. Finally, the main conclusions are summarized.

## 2. MODEL AND SIMULATION METHOD

In this work, we used a coarse-grained model to study the self-assembly of semiflexible homopolymers anchored onto a substrate. The dimensions of the box were set to  $80 \times 80 \times 80$ , and the periodic boundary conditions were applied in the  $x$  and  $y$  directions. First, a rigid array of particles was constructed at the bottom of the box to represent the substrate. Semiflexible homopolymer molecules ( $n = 1024$ ) were then regularly anchored on the substrate at one end and free at the other. Semiflexible homopolymers are represented by a bead–spring model, namely, the molecule chain is constructed by connecting  $N_{\text{bead}}$  beads via harmonic bonds. For the polymers, the positions of the first and the second beads at the anchored end were kept fixed.

The nonbonded potential energy is assumed to be pairwise additive according to

$$U_{\text{nonbond}} = \sum_{i < j} u(r_{ij}) \quad (1)$$

For nanoscale fibers, experimental research<sup>37</sup> showed that adhesion between them can be affected by many factors, such as mechanical interlock, adsorption, chemisorption, electrostatics, and diffusion. In this work, we used the Lennard-Jones (LJ)

potential, which is often used in coarse-grained models,<sup>38–42</sup> to model the attractive interaction between two beads,

$$u(r_{ij}) = \begin{cases} 4\epsilon \left[ \left( \frac{\sigma}{r_{ij}} \right)^{12} - \left( \frac{\sigma}{r_{ij}} \right)^6 \right], & r_{ij} \leq r_c \\ 0, & r_{ij} > r_c \end{cases} \quad (2)$$

where  $r_{ij}$  is the distance between beads  $i$  and  $j$ ,  $r_c = 8.0\sigma$  represents the cutoff radius, and  $\sigma$  and  $\epsilon$  are the length and energy parameters. To represent a strong attractive interaction between beads of homopolymers, we varied  $\epsilon_b = 10\epsilon$  to  $\epsilon_b = 100\epsilon$ , while  $\sigma_b$  was set to  $\sigma$ . Therefore, adhesion between different homopolymers, namely, the inter-homopolymer attraction, is represented by the energy parameter for the interbead interaction,  $\epsilon_b$ . The LJ reduced units were used in this work, and the natural units for our simulations are the diameter of a bead,  $\sigma$ , the mass of a bead,  $m$ , and the LJ well depth,  $\epsilon$ .

In this work, two neighboring beads in a semiflexible homopolymer chain were connected by a harmonic bond potential energy, which is expressed as

$$E_{\text{bond}} = K_{\text{bond}} \sum_{i=1}^{N_{\text{bead}}-1} (r_i - r_{\text{eq}})^2 \quad (3)$$

where  $r_i$  is the distance between neighboring beads  $i$  and  $i+1$ , and  $K_{\text{bond}}$  and  $r_{\text{eq}}$  were set to 800.0 and 1.0 in this work, respectively.  $N_{\text{bead}}$  is the number of beads for a semiflexible homopolymer molecule.

The intrinsic bending stiffness of a semiflexible homopolymer chain was regulated by a harmonic bond angle potential

$$E_{\text{angle}} = K_{\text{angle}} \sum_{i=1}^{N_{\text{bead}}-2} (\theta_i - \theta_{\text{eq}})^2 \quad (4)$$

where  $\theta_i$  is the bond angle formed by three connecting beads and  $\theta_{\text{eq}} = \pi$  is the equilibrium bond angle. The strength of the bond

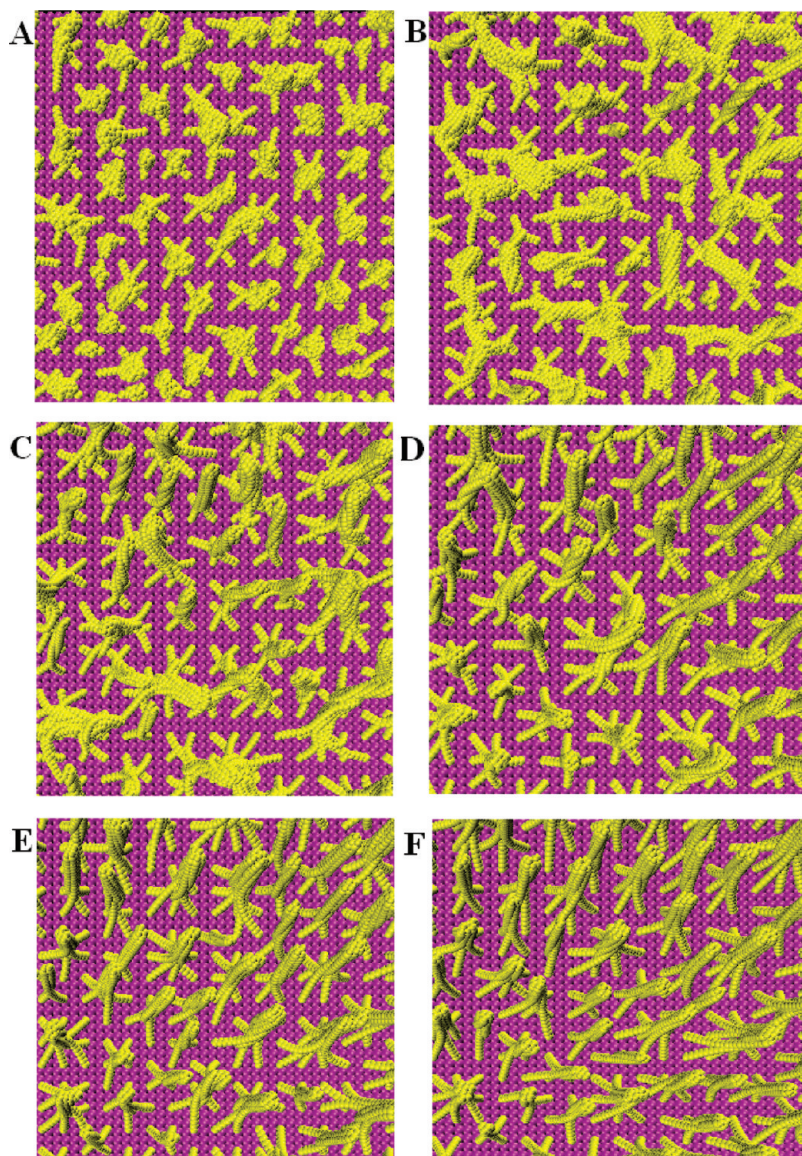


**Figure 2.** Typical snapshots of the self-assembly of flexible homopolymers anchored on a substrate for different values of intrinsic bending stiffness,  $K_{\text{angle}}$ : (A) 20.0, (B) 60.0, (C) 200.0, (D) 500.0, (E) 1000.0, and (F) 5000.0. The molecule length  $N_{\text{bead}}$  and the interaction strength  $\varepsilon_b$  were set to 20 and 30.0, respectively. In order to illustrate the morphology more clearly, only part of the whole morphology is displayed.

angle potential,  $K_{\text{angle}}$ , determines the bending stiffness of homopolymer molecules.

The beads in our model can represent either actual chemical groups of synthetic polymers or larger segments of biopolymers, for example, helical repeat units in actin filaments. Thus, the conversion between the physical length and the dimensionless simulation units depends on the coarse-grained level. If we take 5 nm as a bead size, an approximate size for a G-actin monomer, the length of the semiflexible polymer is about 200 nm. We must note that with such simplified models, semiflexible homopolymers in our work are not restricted to any specific system but instead pertain to a general class of nanoscale fibers. Although the simplicity of our molecular models prevents a quantitative comparison with experiments,<sup>33</sup> a systematic study of such a simple model can provide insight into how the inter-homopolymer attraction and the bending stiffness of homopolymers are combined to control the self-organization of semiflexible homopolymers into ordered structures.

The Brownian dynamics (BD) simulation method was used in this work. In the BD method, the equation of motion for each bead  $i$  is described by

$$m_i v_i(t) = -m_i \xi_i v_i(t) + F_i(x_i(t)) + R_i(t) \quad (5)$$

where  $m_i$ ,  $x_i$ ,  $v_i$  are the mass, position, and velocity of the bead  $i$ , respectively, and  $\xi_i$  is the friction coefficient.  $F_i$  and  $R_i$  are, respectively, the non-hydrodynamic force and random force. Note that in this work the reduced temperature,  $T^* = k_B T / \varepsilon$ , was set to 1.0.

### 3. SIMULATION RESULTS AND DISCUSSION

**3.1. Self-Assembly Patterns: Bundling and Helical Bundling.** To investigate the self-assembly pattern for semiflexible homopolymers anchored on a substrate, we first simulated a small system having only four polymer molecules. In the simulations, we

first set  $N_{\text{bead}} = 30$  and  $\varepsilon_b = 30.0$ , while the bending stiffness of the semiflexible homopolymers was changed from  $K_{\text{angle}} = 20.0$  to  $K_{\text{angle}} = 2000.0$ . In experimental studies, the intrinsic stiffness of a nanoscale fiber can be tuned by changing its geometry, modulus, and aspect ratio.<sup>34</sup> Our simulation results show a trend that helical bundles appear for semiflexible homopolymers having an intermediate bending stiffness (Figure 1C–E), whereas disordered semispherical structures are formed for homopolymers with a low stiffness (Figure 1A,B), and parallel (nonhelical but ordered) bundles structure for those with a high stiffness (Figure 1F).

To illustrate the relationship between the intrinsic bending stiffness and the self-assembly pattern, distributions of the angle between the bond connecting two neighboring beads of a homopolymer and the  $z$ -axis are given in Figure 1M. As expected, the disordered semispherical structure at  $K_{\text{angle}} = 20.0$  shows a broad distribution of the angle over the range of  $(0, \pi/2)$ . At  $K_{\text{angle}} = 2000.0$ , however, a sharp peak for the angle distribution close to zero appears, corresponding to the formation of ordered, parallel bundles (Figure 1M), whereas at  $K_{\text{angle}} = 500.0$ , a moderate peak for the angle distribution appears, indicating the formation of helical bundles.

We also varied  $\varepsilon_b$  to search different patterns with  $N_{\text{bead}} = 30$  and  $K_{\text{angle}} = 500.0$ . Note that the interaction strength between nanoscale bristles can be modified experimentally by using plasma treatment or chemical functionalization,<sup>34</sup> whereas the interaction strength between actin filaments in living cells is mainly modulated by the concentration of cross-linkers.<sup>27–29</sup> Our simulation results show that, for the semiflexible homopolymers, the increase of inter-homopolymer attraction results in the sequential occurrence of parallel bundles (Figure 1G,H) and helical bundles (Figure 1I–L). The distribution of the angle between the bond connecting two neighboring beads of a homopolymer molecule and the  $z$ -axis (Figure 1N) also confirms the occurrence of ordered structures.

In general, different self-assembly patterns, including disordered semispherical clusters, highly ordered helical bundles, and parallel bundles, were observed from our simulations. These primary simulations also indicate that the intrinsic bending stiffness and inter-homopolymer attraction significantly affect the self-assembly pattern. This observation is in agreement with previous experimental investigations.<sup>27–29,33–35</sup> For example, the intrinsic bending stiffness of nanoscale bristles was proved to play a significant role for the final self-assembly pattern.<sup>33–35</sup> The concentration of cross-linkers, which modulated the interaction strength between actin filaments, significantly affects characteristic structural motifs of actin filaments.<sup>27–29</sup> In addition, experimental investigations have suggested that the length of bristles and that of actin filaments play an important role in their clustering.<sup>26,33,34</sup> To understand the molecular mechanism of bundling and helical bundling of semiflexible homopolymers, below we investigate the effects of  $K_{\text{angle}}$ ,  $N_{\text{bead}}$ , and  $\varepsilon_b$  on the self-assembly patterns in detail.

**3.1.1. Effects of the Intrinsic Bending Stiffness of Semiflexible Homopolymers.** In order to investigate the effect of intrinsic bending stiffness on bundling, the bond angle potential parameter,  $K_{\text{angle}}$ , was altered while the interaction strength and molecule length were fixed to 30.0 and 20, respectively. In order to produce reasonable statistics of self-assembly patterns, a larger simulation system is necessary in this work. Here, a larger simulation box of  $80 \times 80 \times 80$  was chosen to represent a larger system with 1024 semiflexible homopolymer molecules.

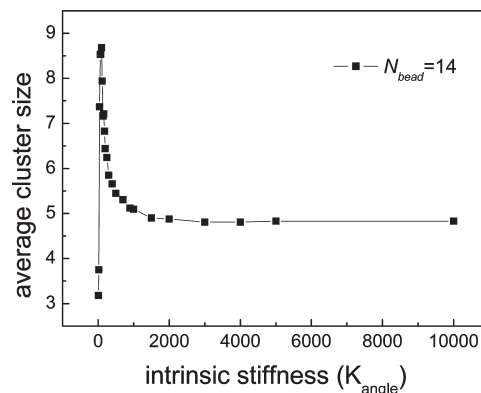


**Figure 3.** Average cluster size as a function of the intrinsic bending stiffness. The molecule length  $N_{\text{bead}}$  and interaction strength  $\varepsilon_b$  were set to 14 and 30.0, respectively.

Several typical snapshots and average cluster sizes are shown in Figure 2 and Figure 3, respectively, as a function of  $K_{\text{angle}}$ . In general, as  $K_{\text{angle}}$  increases gradually, semiflexible homopolymers tend to self-assemble into disordered clusters, highly ordered helical bundles, and parallel bundles, sequentially (Figure 2). At the same time, the average cluster size of the assemblies changes non-monotonously with increasing  $K_{\text{angle}}$  (Figure 3). The largest bundle is obtained at  $K_{\text{angle}} \sim 100.0$ , which divides the whole range of the bending stiffness values into three regions.

In the region of  $K_{\text{angle}} \leq 100.0$ , the average cluster size rapidly increases from 3.2 to 8.7 as  $K_{\text{angle}}$  increases. This is because when semiflexible homopolymers are rather flexible, e.g.,  $K_{\text{angle}} = 20.0$ , the homopolymers collapse down to the substrate and form semispherical aggregates rather than homopolymer bundles (Figure 2A). Furthermore, the formation of the disordered clusters inhibits their combination with other clusters to form a larger one. In the region of  $K_{\text{angle}} \leq 100.0$ , the increase of  $K_{\text{angle}}$  causes the clusters to stand up (Figure 2B) and thus induce the increase in cluster size (Figure 3).

However, for  $100.0 \leq K_{\text{angle}} \leq 1000.0$ , the increase of  $K_{\text{angle}}$  results in the decrease in bundle size from 8.7 to 5.1. In this region, the self-assembly of homopolymers is sensitive to  $K_{\text{angle}}$ , namely, the bending stiffness of homopolymers, whereas further increasing  $K_{\text{angle}}$  from 1000.0 does not induce an obvious decrease in the average cluster size. In other words, for the region of  $K_{\text{angle}} > 1000.0$ , the self-assembly of homopolymers is insensitive to the bending stiffness. A detailed inspection of Figure 2 indicates that patterns of helical bundles are formed for  $100.0 < K_{\text{angle}} < 1000.0$  and parallel bundles for  $K_{\text{angle}} > 1000.0$ . Although the increase of  $K_{\text{angle}}$  in the region of  $K_{\text{angle}} > 1000.0$  does not induce an obvious decrease in the average cluster size (Figure 3), the contact area between adjacent semiflexible homopolymers in each bundle gradually decreases, indicating the continuous transition of the bundles from helical to nonhelical ones.

**3.1.2. Effects of the Molecule Length of Semiflexible Homopolymers.** In order to investigate the effects of the molecule length of semiflexible homopolymers,  $N_{\text{bead}}$  was altered from 6 to 40 in a number of independent simulation runs, while  $\varepsilon_b$  and  $K_{\text{angle}}$  were fixed to 30.0 and 500.0, respectively. Again, a larger simulation system of  $80 \times 80 \times 80$  was adopted to obtain a good statistics. Our simulations indicate that the molecule length plays an important role in the self-assembly pattern (Figure 4). Obviously, longer homopolymer molecules tend to form larger

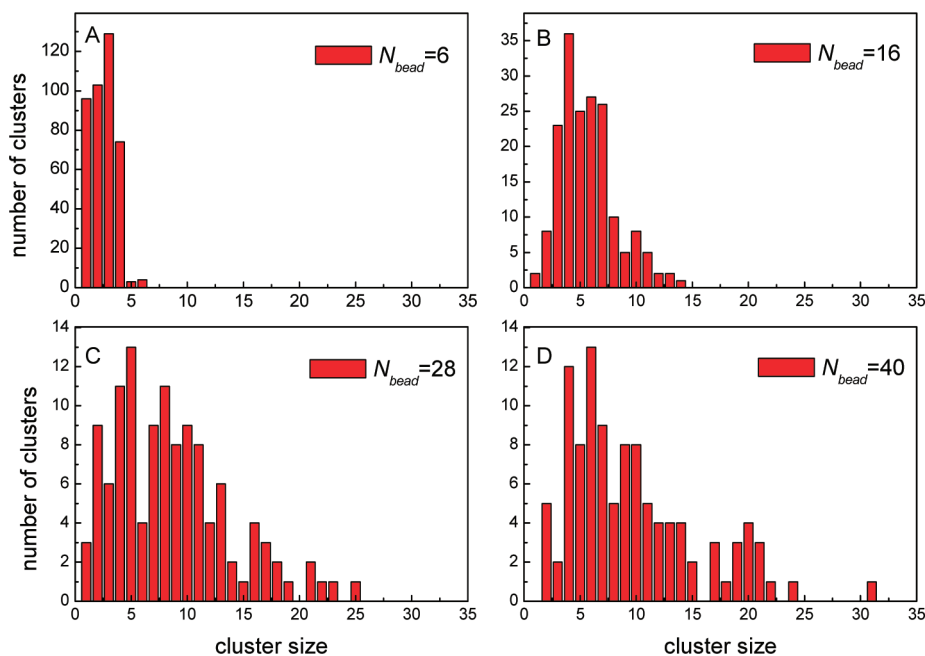


**Figure 4.** Cluster size distributions for the systems with different molecule lengths. Note that  $K_{\text{angle}}$  and  $\varepsilon_b$  were set to 500.0 and 30.0, respectively.

clusters (Figure 4C,D) because of their larger aspect ratio. For shorter homopolymers, on the contrary, they tend to form smaller clusters.

To illustrate the effects of molecule length in more detail, the average cluster size as a function of molecule length,  $N_{\text{bead}}$ , is given in Figure 5A. To obtain good statistics, cluster sizes for each chain length were averaged over at least 10 independent runs in the same thermodynamic conditions. The statistical uncertainties in the figure were obtained as the standard deviations of the results from those independent runs. Unexpectedly, the average cluster size does not increase linearly with  $N_{\text{bead}}$  but shows a stepwise manner. For the first step, the average cluster size first notably increases with the chain length ( $N_{\text{bead}} < 10$ ), and then slows down until the length reaches another critical value ( $N_{\text{bead}} > 10$ ). We ascribe the stepwise increase of cluster size to the existence of two different bundling mechanisms. One is the direct bundling of several single semiflexible homopolymers, and the other is the combination of several small bundles into a larger one.<sup>26,33,34</sup>

The existence of different bundling mechanisms can be proved by the bundling dynamics. The bundling dynamics (Figure 5B) indicates that for short polymers ( $N_{\text{bead}} < 10$ ), the direct bundling of several single semiflexible homopolymers is controlled by the frequent exchange of individual polymers. In this case, the exchange of individual polymers is confirmed by the obvious fluctuation of the number of free monomers (Figure 5B). Therefore, for short polymers, the initial dramatic increase of the average cluster size in Figure 5A is mainly ascribed to the increase of molecule length.

For long polymers ( $N_{\text{bead}} > 10$ ), however, the fluctuation of free monomers is strongly suppressed after the initial formation of small clusters (Figure 5B). Therefore, it is the fusion of small clusters rather than the exchange of individual polymers controlling the bundling dynamics. In this case, the formation of small bundles also increases the bending stiffness of the homo-polymer bundles, which in turn inhibits the fusion of two adjacent bundles. As a result, the growth rate of the cluster size significantly

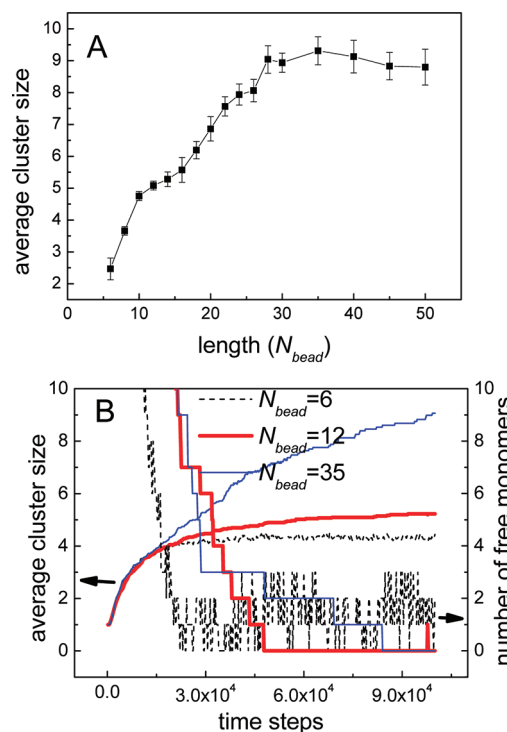


**Figure 5.** (A) Average cluster size as a function of molecule length  $N_{\text{bead}}$ . Note that  $K_{\text{angle}}$  and  $\varepsilon_b$  were set to 500.0 and 30.0, respectively. (B) The corresponding evolution of the number of free monomers and that of average cluster size. Note that the data are obtained from a single simulation.

slows down after the initial formation of small clusters (Figure 5B). This is also one of the reasons that when the chain length is larger than 30, a further increase of chain length would not increase the cluster size. Another reason for the appearance of second step

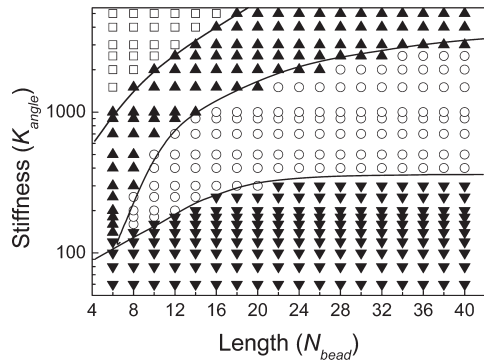


**Figure 6.** Morphology diagram for the self-assembly of semiflexible homopolymers in the  $K_{\text{angle}} - N_{\text{bead}}$  plane for the case of  $\epsilon_b = 30.0$ . The symbol  $\square$  represents the pattern composed of unclustered homopolymers,  $\blacktriangle$  represents the parallel bundles,  $\circ$  represents the helical bundles, and  $\blacktriangledown$  represents the disordered clusters. The solid lines are included as a guide for the eye.

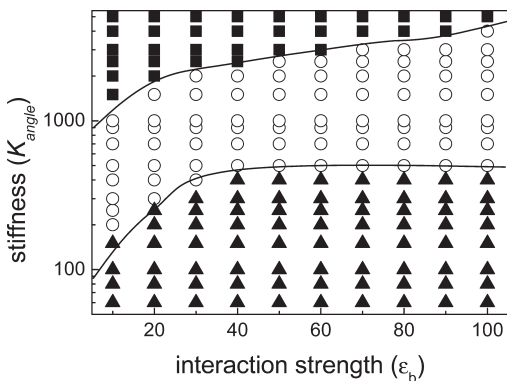


**Figure 7.** The morphology diagram in the plane ( $K_{\text{angle}}, \epsilon_b$ ) for the case of  $N_{\text{bead}} = 30$ . Three different assembly morphologies are observed: ( $\blacksquare$ ) parallel bundles, ( $\circ$ ) helical bundles, and ( $\blacktriangle$ ) disordered clusters. The solid lines are included as a guide for the eye.

( $N_{\text{bead}} > 30$ ) is that the short-range interaction we used in this work decays rapidly as the separation between neighboring clusters increases.

We also investigated the effect of  $\epsilon_b$  on the self-assembly patterns of semiflexible homopolymers. The simulation results indicate that the different values of the inter-homopolymer attraction may cause the occurrence of different self-assembly patterns, which will be discussed below.

**3.1.3. Morphology Diagrams.** Previous experimental investigations proved that the helical assembly of anchored nanoscale bristles is the result of competition between capillary force and intrabristle elasticity.<sup>33,34</sup> Nevertheless, the mechanism of helical bundling, especially the effects of various factors, such as the bristle length and its intrinsic bending stiffness, has not been thoroughly understood. Our simulations demonstrate that the extent of bundling and that for helical bundling are strongly affected by the intrinsic bending stiffness of semiflexible homopolymers, inter-homopolymer attraction, and molecule length. To illustrate further how the different factors cooperatively determine the self-assembly pattern, we performed extensive simulations to determine the morphology diagrams.

Figure 6 gives the detailed morphology diagram in the  $K_{\text{angle}} - N_{\text{bead}}$  plane when the interaction strength  $\epsilon_b$  was set to 30.0.

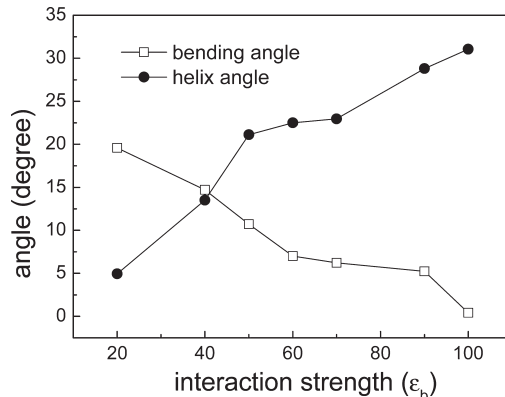


**Figure 8.** Helix angle of the bundle as a function of interaction strength and the bending angle of the bundle responding to a fixed lateral force exerted on its free end.  $N_{\text{bead}}$  and  $K_{\text{angle}}$  were set to 30 and 1000.0, respectively. The average bending angle for isolated homopolymers is  $66.14^\circ$ .

The figure shows that four different self-assembly patterns exist, including patterns with unclustered homopolymers, disordered semispherical clusters, ordered helical bundles, and parallel bundles. As expected, the unclustered patterns are observed for homopolymers with a short molecule length and high stiffness, and disordered structures are formed by homopolymers with a low stiffness. Bundling and helical bundling can only occur for homopolymers with a sufficient molecule length and intermediate bending stiffness, consistent with conclusions from Figures 1, 3, and 4. Moreover, the occurrence of helical bundling requires a weaker bending stiffness.

The morphology diagram in the plane ( $K_{\text{angle}}, \epsilon_b$ ) is given in Figure 7 for the case of  $N_{\text{bead}} = 30$ . From the figure, only three self-assembly patterns, including disordered clusters, ordered helical bundles, and parallel bundles, are observed. The formation of helical bundles is found to be controlled by the balance between the interaction strength and the bending stiffness. For semiflexible homopolymers with a high stiffness, a strong inter-homopolymer attraction is required to generate the structure of helical bundles (Figure 7), whereas for homopolymers with a weak stiffness, the strong inter-homopolymer attraction tends to result in a disordered structure rather than an ordered helical bundle (Figure 7).

**3.2. Stiffness Enhancement by Helical Bundling.** In biology, the bending stiffness of actin bundles plays an important role in many cellular activities, such as cellular fission, endocytosis, and cell movement.<sup>43</sup> Therefore, understanding how the stiffness changes as the formation of helical bundles is of biological significance. Here, we demonstrated the reinforcement of the bending stiffness of a bundle induced by helical bundling. First, a number of homopolymer bundles composed of four semiflexible homopolymer molecules ( $K_{\text{angle}} = 1000.0$ ) were prepared, in which the helical extent of bundles was regulated by the interaction strength. Figure 8 shows that the helix angle increases with the strength of the inter-homopolymer attraction. This observation is in agreement with our conclusion from Figure 7. Then, a fixed lateral force was exerted on the free end of the homopolymers. Simulation results show that the bending angle decreases as the helical extent increases (Figure 8). Because the bending stiffness of the bundle can be reflected by its bending angle responding to the exerted force, this observation indicates that the helical bundling enhances the bending stiffness of the bundle.

As a comparison, we also performed a simulation in which the semiflexible homopolymers were separated from each other (without the formation of homopolymer bundle), and the total lateral force was evenly distributed on the free end of the isolated homopolymers. The average bending angle for the isolated homopolymers is  $66.14^\circ$ , much larger than the largest bending angle of  $22.5^\circ$  for homopolymer bundles. This observation and that in Figure 8 prove the bundling-induced stiffness enhancement. In general, the bundle formation reinforces the bending stiffness, and the stiffness is furthermore enhanced by the helical bundling.

**3.3. Scaling Analysis of Helical Bundling.** In this work, a simple scaling analysis is presented to understand the helical bundling. In a minimal model, two initially straight homopolymers wind around each other to form uniform helices of pitch  $p$  and radius  $r$ . A helix then can be described parametrically by the following equations:

$$\begin{cases} x = r \cos t \\ y = r \sin t \\ z = ct \end{cases} \quad (6)$$

with  $c = p/2\pi$ . Therefore, the curvature of the helix is determined by  $k = r/(r^2 + c^2)$ , and the arc length per pitch is  $L_{\text{arc}} = 2\pi(c^2 + r^2)^{1/2}$ . The adhesion energy in the arc length can be written as

$$U_{\text{adhesion}} = \sum_{N_{\text{arc}}} U_{ij} \sim N_{\text{arc}} U_{\text{LJ}}^{\min} \sim L_{\text{arc}} \varepsilon_b \sim (c^2 + r^2)^{1/2} \varepsilon_b \quad (7)$$

with the number of beads in one helical repeat  $N_{\text{arc}} \sim L_{\text{arc}}$  and the minimum of LJ potential  $U_{\text{LJ}}^{\min} \sim \varepsilon_b$  (see eq 2). On the other hand, the bending energy of two homopolymers is  $U_{\text{bending}} = \sum_{N_{\text{arc}}} 2K_{\text{angle}}(\theta - \pi)^2 \sim N_{\text{arc}} K_{\text{angle}}(\theta - \pi)^2 \sim L_{\text{arc}} K_{\text{angle}}(\theta - \pi)^2 \sim (c^2 + r^2)^{1/2} K_{\text{angle}}(\theta - \pi)^2$ . As  $(\theta - \pi) \sim r/(r^2 + c^2)$ , we get

$$U_{\text{bending}} \sim K_{\text{angle}} r^2 (r^2 + c^2)^{-3/2} \quad (8)$$

Therefore, the total energy of our system  $U_{\text{total}}$  is given by

$$U_{\text{total}} \sim \lambda \varepsilon_b (c^2 + r^2)^{1/2} + K_{\text{angle}} r^2 (r^2 + c^2)^{-3/2} \quad (9)$$

with  $\lambda$  as a constant. Here, the minimization of the total energy requires  $\partial U_{\text{t}}/\partial c = 0$ , from which we get

$$K_{\text{angle}}/\varepsilon_b \sim (r^2 + c^2)^2/r^2 \sim ((2\pi r)^2 + p^2)^2/r^2 \quad (10)$$

According to eq 10, for strongly stiff homopolymers, namely,  $\varepsilon_b/K_{\text{angle}} \ll 1$ , the two homopolymers favor parallel bundles ( $p \rightarrow \infty$ ) (Figure 1F), whereas for rather flexible homopolymers ( $\varepsilon_b/K_{\text{angle}} \gg 1$ ), they favor bundling with the pitch as small as possible, which may be achieved by disordered semispherical clusters (Figure 1A). The equation also indicates that the helix angle increases with the strength of the inter-homopolymer attraction or with decreasing intrinsic bending stiffness, being consistent with Figures 1 and 8, respectively. In general, the scaling analysis again demonstrates that the formation of helical structures is controlled by the balance between the inter-homopolymer attraction and the bending stiffness, in qualitative agreement with our simulation results.

**3.4. Bundling Dynamics.** In this section, we investigated the bundling dynamics of semiflexible homopolymers anchored on a substrate. From our simulations, two bundling pathways were

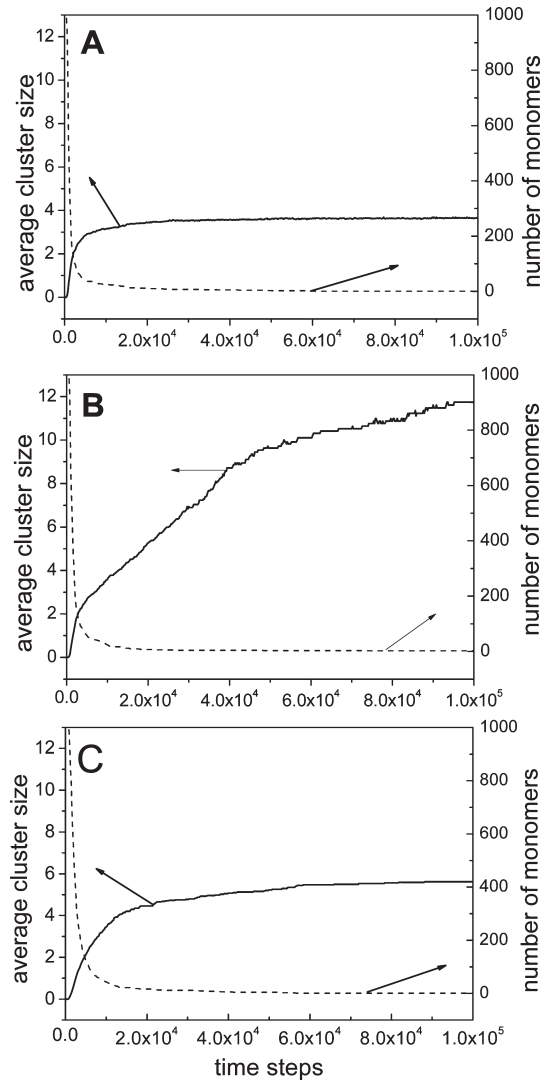


**Figure 9.** Time evolution of the number of monomers and that of average cluster size of anchored homopolymers with different intrinsic bending stiffness values: (A) 10.0, (B) 80.0, and (C) 5000.0. The molecule length  $N_{\text{bead}}$  and interaction strength  $\varepsilon_b$  were fixed to 24 and 60.0.

identified: hierarchical bundling and nonhierarchical bundling. Note that hierarchical assembly is abundant in nature, e.g., the hierarchical helical assembly of mesoscale bristles driven by capillary force.<sup>33,34</sup> Several examples of the bundling dynamics are displayed in Figures 5B and 9A–C. Here, we recognized a bundling process to be dynamically hierarchical when the time evolution of average cluster size obviously lags behind that of the number of monomers (see Figure 9B as an example). In other words, for a process of hierarchical bundling, the cluster growth and monomer consumption are asynchronous to each other. Otherwise, the bundling process is nonhierarchical (see Figure 9A, C). Figure 9 indicates that hierarchical bundling can occur for homopolymers with an intermediate bending stiffness (such as  $K_{\text{angle}} = 80.0$  in Figure 9B).

For rather flexible homopolymers, disordered clusters, which are approximately semispherical, are immediately formed once several homopolymers come in contact with each other (Figure 1A). The initial formation of the well-separated clusters prevents them from self-assembling into larger clusters, giving rise to a

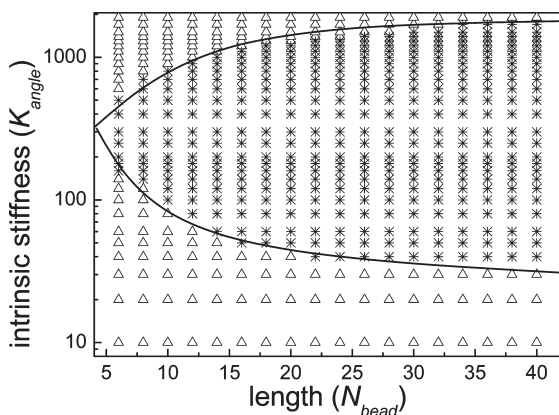


**Figure 10.** Two distinct bundling dynamics for  $\varepsilon_b = 60.0$ : (\*) hierarchical assembly and ( $\Delta$ ) nonhierarchical assembly. The solid lines are included as a guide for the eye.

nonhierarchical bundling process (Figure 9A). However, a moderate increase in bending stiffness has been proved to induce the transition from disordered clusters to highly ordered helical bundles (Figure 7). In this case, the adjacent bundles with a moderate stiffness may further aggregate to form a larger bundle and hence result in hierarchical bundling. This is the reason that the evolution of average cluster size significantly lags behind that of the number of monomers (Figure 9B). But for a large value of  $K_{\text{angle}}$ , the stiffness of the whole bundle strongly increases so that the hierarchical bundling is inhibited (Figure 9C).

Similar to the effects of  $K_{\text{angle}}$  on the bundling dynamics, it is reasonable to assume that the hierarchical bundling can only occur for relatively longer homopolymers. This assumption is confirmed by Figure 10, in which the assembly pathways including hierarchical and nonhierarchical bundling are extensively determined and summarized in the  $K_{\text{angle}} - N_{\text{bead}}$  plane. The figure clearly illustrates that the hierarchical bundling only occurs for long homopolymers with an intermediate intrinsic bending stiffness.

#### 4. CONCLUSIONS

In this work, we investigated how the self-assembly of semiflexible homopolymers anchored on a substrate is controlled by several intrinsic features of the homopolymers, including the molecule length, the intrinsic bending stiffness, and the attraction between different homopolymer molecules. For final self-assembly structures, four different patterns, including patterns with unclustered homopolymers, disordered semispherical clusters, ordered helical bundles, and parallel (nonhelical but ordered) bundles, were observed from our simulations. We focused on the formation mechanism of the stable bundles and that for the helical structures. Simulation results show that bundling can only occur for the semiflexible homopolymers with a sufficient molecule length and intermediate bending stiffness. However, the formation of helical structures is controlled by the balance between the inter-homopolymer attraction and the bending stiffness. For semiflexible homopolymers with a high stiffness, a strong inter-homopolymer attraction is required to generate the structure of helical bundles, whereas for homopolymers with a weak stiffness, the strong inter-homopolymer attraction tends to result in the disordered semispherical structure rather than ordered bundles. Furthermore, our simulations demonstrated that the

bundle formation reinforces the bending stiffness, and the stiffness is further enhanced by helical bundling.

For the dynamic aspect, both hierarchical bundling and nonhierarchical bundling were observed. Simulation results indicate that the hierarchical bundling only occurs for long homopolymers with an intermediate intrinsic bending stiffness. In general, our results provide a practical guide to control the final patterns and assembly dynamics of semiflexible homopolymers when generating diverse structures. Moreover, the study on the structural and dynamic properties on the self-organization of semiflexible polymers would contribute to our understanding of the functioning of the cytoskeleton.

#### ■ AUTHOR INFORMATION

##### Corresponding Author

\*E-mail: zhangxr@mail.buct.edu.cn.

#### ■ ACKNOWLEDGMENT

This work was financially supported by the National Natural Science Foundation of China (No. 20736005 and No. 20876004).

#### ■ REFERENCES

- (1) Lichtenegger, H.; Müller, M.; Paris, O.; Riekel, C.; Fratzl, P. *J. Appl. Crystallogr.* **1999**, *32*, 1127.
- (2) Wagermaier, W.; Gupta, H. S.; Gourrier, A.; Burghammer, M.; Roscher, P.; Fratzl, P. *Biointerfaces* **2006**, *1*, 1.
- (3) Weiner, S.; Wagner, H. D. *Annu. Rev. Mater. Sci.* **1998**, *28*, 271.
- (4) Essner, J. J.; Vogan, K. J.; Wagner, M. K.; Tabin, C. J.; Yost, H. J.; Brueckner, M. *Nature* **2002**, *418*, 37.
- (5) Rubin, N.; Perugia, E.; Goldschmidt, M.; Fridkin, M.; Addadi, L. *J. Am. Chem. Soc.* **2008**, *130*, 4602.
- (6) Holmes, K. C.; Popp, D.; Gebhard, W.; Kabsch, W. *Nature* **1990**, *347*, 44.
- (7) Chouaib, N.; Goriely, A.; Maddocks, J. H. *Proc. Natl. Acad. Sci. U. S. A.* **2006**, *103*, 9398.
- (8) Wang, J.; Feng, X.; Wang, G.; Yu, S. *Appl. Phys. Lett.* **2008**, *92*, 191901.
- (9) Snir, Y.; Kamien, R. D. *Science* **2005**, *307*, 1067.
- (10) Han, Y.; Zhao, L.; Ying, J. Y. *Adv. Mater.* **2007**, *19*, 2454.
- (11) Kudlay, A.; Cheung, M. S.; Thirumalai, D. *Phys. Rev. Lett.* **2009**, *102*, 118101.
- (12) Christopoulos, D. K.; Terzis, A. F.; Vanakaras, A. G.; Photinos, D. J. *J. Chem. Phys.* **2006**, *125*, 204907.
- (13) Snir, Y.; Kamien, R. D. *Phys. Rev. E: Stat., Nonlinear, Soft Matter Phys.* **2007**, *75*, 051114.
- (14) Pickett, G. T.; Gross, M.; Okuyama, H. *Phys. Rev. Lett.* **2000**, *85*, 3652.
- (15) Troche, K. S.; Coluci, V. R.; Braga, S. F.; Chinellato, D. D.; Sato, F.; Lugoas, S. B.; Rurrali, R.; Galvao, D. S. *Nano Lett.* **2005**, *5*, 349.
- (16) Yin, Y.; Xia, Y. *J. Am. Chem. Soc.* **2003**, *125*, 2048.
- (17) Zhang, X.; Cao, D.; Wang, W. *J. Phys. Chem. C* **2007**, *112*, 2943.
- (18) Yue, T.; Jiang, G.; Zhang, X. *Phys. Chem. Chem. Phys.* **2011**, *13*, 12497.
- (19) Li, H.; Li, Y. F.; Liew, K. M.; Zhang, J. X.; Liu, X. F. *Appl. Phys. Lett.* **2009**, *95*, 183101.
- (20) Rafelski, S. M.; Theriot, J. A. *Annu. Rev. Biochem.* **2004**, *73*, 209.
- (21) Balaban, N. Q.; Schwarz, U. S.; Riveline, D.; Goichberg, P.; Tzur, G.; Sabanay, I.; Mahalu, D.; Safran, S.; Bershadsky, A.; Addadi, L.; Geiger, B. *Nat. Cell Biol.* **2001**, *3*, 466.
- (22) Geiger, B.; Spatz, J. P.; Bershadsky, A. D. *Nat. Rev. Mol. Cell Biol.* **2009**, *10*, 21.
- (23) Puklin-Faucher, E.; Sheetz, M. P. *J. Cell Sci.* **2009**, *122*, 179.

- (24) Wehrle-Haller, B.; Imhof, B. A. *Int. J. Biochem. Cell Biol.* **2003**, 35, 39.
- (25) Haviv, L.; Brill-Karniely, Y.; Mahaffy, R.; Backouche, F.; Ben-Shaul, A.; Pollard, T. D.; Bernheim-Groswasser, A. *Proc. Natl. Acad. Sci. U. S. A.* **2006**, 103, 4906.
- (26) Brill-Karniely, Y.; Ideses, Y.; Bernheim-Groswasser, A.; Ben-Shaul, A. *ChemPhysChem* **2009**, 10, 2818.
- (27) Tempel, M.; Isenberg, G.; Sackmann, E. *Phys. Rev. E: Stat., Nonlinear, Soft Matter Phys.* **1996**, 54, 1802.
- (28) Pelletier, O.; Pokidysheva, E.; Hirst, L. S.; Bouxsein, N.; Li, Y.; Safinya, C. R. *Phys. Rev. Lett.* **2003**, 91, 148102.
- (29) Gardel, M. L.; Shin, J. H.; MacKintosh, F. C.; Mahadevan, L.; Matsudaira, P.; Weitz, D. A. *Science* **2004**, 304, 1301.
- (30) Kierfeld, J.; Kühne, T.; Lipowsky, R. *Phys. Rev. Lett.* **2005**, 95, 038102.
- (31) Shin, H.; Drew, K. R. P.; Bartles, J. R.; Wong, G. C. L.; Grason, G. M. *Phys. Rev. Lett.* **2009**, 103, 238102.
- (32) Grason, G. M.; Bruinsma, R. F. *Phys. Rev. Lett.* **2007**, 99, 098101.
- (33) Pokroy, B.; Kang, S. H.; Mahadevan, L.; Aizenberg, J. *Science* **2009**, 323, 237.
- (34) Kang, S. H.; Pokroy, B.; Mahadevan, L.; Aizenberg, J. *ACS Nano* **2010**, 4, 6323.
- (35) Duan, H.; Berggren, K. K. *Nano Lett.* **2010**, 10, 3710.
- (36) Paulose, J.; Nelson, D. R.; Aizenberg, J. *Soft Matter* **2010**, 6, 2421.
- (37) Lu, Y.; Huang, J. Y.; Wang, C.; Sun, S.; Lou, J. *Nat. Nanotechnol.* **2010**, 6, 218.
- (38) Zhang, Z.; Horsch, M. A.; Lamm, M. H.; Glotzer, S. C. *Nano Lett.* **2003**, 3, 1341.
- (39) Zhang, Z.; Glotzer, S. C. *Nano Lett.* **2004**, 4, 1407.
- (40) Horsch, M. A.; Zhang, Z.; Glotzer, S. C. *Phys. Rev. Lett.* **2005**, 95, 056105.
- (41) Horsch, M. A.; Zhang, Z.; Glotzer, S. C. *Nano Lett.* **2006**, 6, 2406.
- (42) Singh, C.; Ghorai, P. K.; Horsch, M. A.; Jackson, A. M.; Larson, R. G.; Stellacci, F.; Glotzer, S. C. *Phys. Rev. Lett.* **2007**, 99, 226106.
- (43) Pollard, T. D.; Cooper, J. A. *Science* **2009**, 326, 1208.